Jylhä, Jani-Petteri; Jokilaakso, Ari

CFD-DEM models for matte droplet settling in a flash smelting settler

Published in:
Heliyon

DOI:
10.1016/j.heliyon.2023.e21570

Published: 01/11/2023

Document Version
Publisher's PDF, also known as Version of record

Heliyon 9 (2023) e21570

Contents lists available at ScienceDirect

Heliyon

journal homepage: www.cell.com/heliyon

Research article

CFD-DEM models for matte droplet settling in a flash smelting settler

Jani-Petteri Jylhä, Ari Jokilaakso *

Aalto University, School of Chemical Engineering, Department of Chemical and Metallurgical Engineering, Kemistintie 1, Espoo, 02150, Finland

ARTICLE INFO

Keywords:
Simulation
Copper
Slag
Coalescence
Reaction kinetics

ABSTRACT

The flash smelting process is widely used in copper production. In the process, sulfidic feed and flux are oxidized. The heat released in the reactions melts the feed which forms a slag layer through which matte droplets must settle. Understanding the different phenomena affecting the settling is important to minimize losses. Due to the high temperature, simulation methods were employed to study settling. In this work, coupled CFD-DEM was used to study the effect of coalescence and reactions with in-house built submodels and scaled-down geometries. Colliding droplets often coalesce into larger droplets while reactions decrease their size and make them denser. These increase the settling velocity which is further enhanced by the formation of a channeling flow. Channels make the droplet cluster denser causing more collisions. This method enables the phenomena to be studied at the individual droplets' details, although simulating a full-scale process is beyond the available computational resources.

1. Introduction

Metso's Outotec Flash Smelting Process is widely used in copper production. In flash smelting, sulfides are oxidized in a smelting feed concentrate forming copper matte. The copper content of the matte is 55 – 70 wt% [1] but the matte also contains sulfur, iron and other impurities [2].

Metso's Outotec flash smelting furnace (FSF) is presented in Fig. 1. The concentrate is oxidized in the reaction shaft and the matte droplets that are formed hit the slag layer in the settler. The matte droplets settle through the slag forming a separate immiscible layer. Droplets react further during settling which removes iron and sulfur from the droplets. Matte is refined to copper in further processing.

The thick walls with cooling elements and high temperatures of 1220-1320 °C [3,4] make in-situ observations of the FSF settler impossible in practice. Thus, the settler has been studied with CFD (computational fluid dynamics) simulations [5–8] but details of the settling phenomenon cannot be studied with CFD as the droplets cannot be individually simulated. New approach has been applied to create more detailed simulations of key phenomena occurring in the settler. In this work, matte settling was studied using coupled CFD-DEM (discrete element method) simulation. The commercial software Ansys Fluent 2021 R1 and Altair EDEM was used for CFD and DEM, respectively. The software was coupled by a plugin provided by Altair EDEM. The simulations were modified by using additional models for DEM. These models simulated coalescence due to droplet collisions and changes in physical properties

* Corresponding author.
E-mail address: ari.jokilaakso@aalto.fi (A. Jokilaakso).

https://doi.org/10.1016/j.heliyon.2023.e21570
Received 3 August 2023; Received in revised form 2 October 2023; Accepted 24 October 2023

Available online 29 October 2023

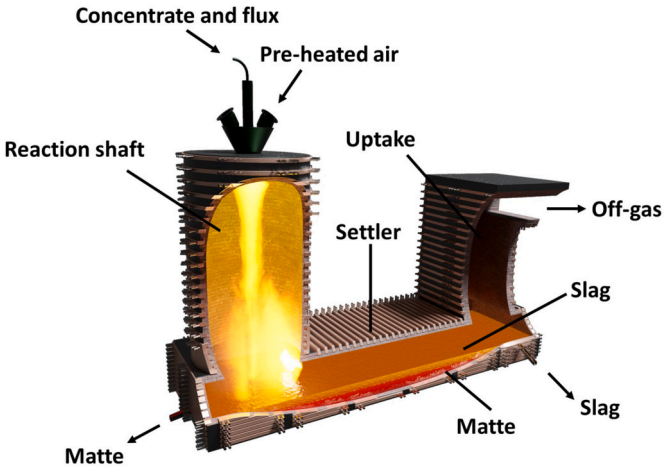

Fig. 1. Outotec flash smelting furnace.

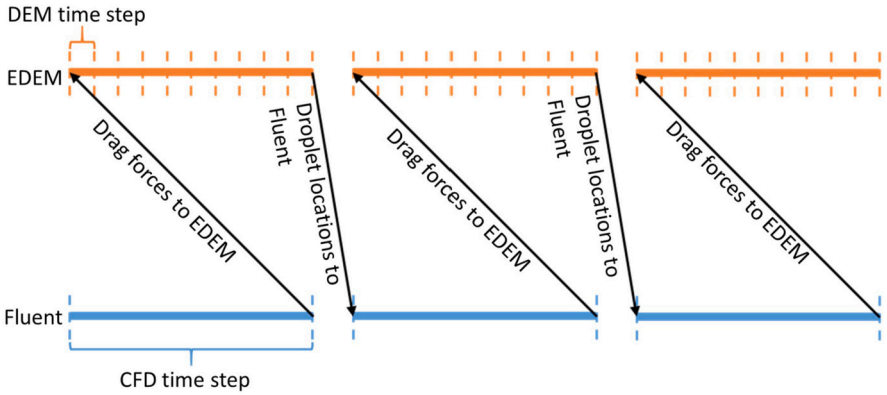

Fig. 2. CFD-DEM calculation process and time steps.

as a result of reactions in the slag. Coalescence and reactions change the droplet size and density, which are the major factors in settling. This paper presents a continuation and improvements on the results originally presented at Copper 2019 [9].

2. Methods

Settling copper matte droplets were simulated using the coupled CFD-DEM method. CFD was used to simulate the slag while DEM was used to simulate each droplet individually as very soft spherical particles. The main function of the simulated slag was to resist the settling of droplets due to drag and to simulate the flows caused by the settling droplets while also allowing the flows to affect them. DEM simulated the effect of gravity on the droplets and also collisions between the droplets, coalescence, and changes in droplet properties due to reactions.

In this CFD-DEM simulation, CFD first simulates the flow in the model for one time step and then DEM simulates particle movement until the end of the CFD time step is reached. Droplet locations and drag forces are transferred when switching to CFD and to DEM, respectively. Typically, the time step is shorter in DEM than in CFD. A depiction of the CFD-DEM calculation process is presented in Fig. 2.

3. Simulations

3.1. Model geometries

Three different model geometries were used to simulate a section of the flash smelting settler under the reaction shaft where droplets hit the slag surface. However, due to the very high demand of computational resources in the CFD-DEM method, the section was heavily scaled down, allowing simulation of settling with affordable settler dimensions and number of droplets.

The simulated geometries were two 8-liter cubic models and a 5-liter tall and narrow rectangular cuboid with realistic slag height. The two cubic models were similar, but one had an inlet and outlet for slag flow while the other simulated a stagnant slag layer. The three different model geometries were named cubic, simple, and deep models for the inlet-outlet, stagnant slag, and tall rectangular

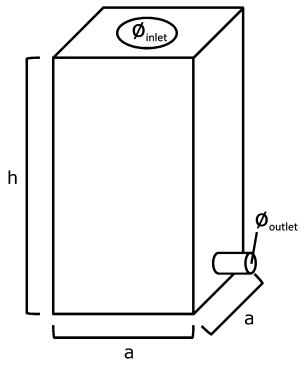

Fig. 3. Sketch of the used geometry.

Table 1
Dimensions of the geometries [mm].

	Cubic/Simple	Deep
h	200	500
a	200	100
$\varnothing_{inlet}$	150	20
$\varnothing_{outlet}$	15	10

Table 2
Slag values used in Fluent.

Parameter	Value
ρ	3150 kg/m^3
μ	0.45 kg/ms
feed_{cubic}	0.022 kg/s
feed_{deep}	0.00038 kg/s
time step	$5 \cdot 10^{-5}$ s

cuboid models, respectively. A diagram of the base geometry is presented in Fig. 3 and the dimensions of the models are presented in Table 1.

The cubic and simple models were used for coalescence while the deep model was used as a combined model including both coalescence and reaction simulation as its depth allowed longer settling times for the matte droplets. Every model had an inlet in the middle of the top surface. However, in the simple model, the inlet was only used for feeding matte droplets. The cubic and deep models also had an outlet at one side, a few centimeters above the bottom of the model. The matte feed of the deep model was significantly decreased to limit the number of droplets in the simulation and, thus, the computation time.

Particles in EDEM were defined by creating a material with the right properties and assigning a particle to it. The particles may be spherical models with single or multi-sphere shapes, polyhedra, or spherocylinders. In these simulations the particles were set as very soft singular spheres. A normal distribution was assigned to control the size distribution of the spheres. The size distribution is calculated by the software using a mean size and setting a scale factor for each created sphere.

3.2. CFD model

All the CFD simulations in this work used a realizable k-ε turbulence model with scalable wall functions. The outlet was set as a pressure outlet. Two-phase EDEM-Fluent coupling uses DDPM (dense discrete phase model) for particles where a spherical drag law is applied as the droplets are assumed to be spheres.

The feed rates for the slag and matte were based on the reported literature values [3]. The slag feed was scaled down using a similar feed rate per unit area. In this case, the relevant areas were the reaction shaft of the reported furnace and the inlet area of the model. The matte feed was set as 40% of the slag feed, as the reported matte production values of the modeled furnace were approximately 40% of the slag production values. The values used in CFD have been presented in Table 2.

As the CFD part of the CFD-DEM simulations was not the main focus of the study, the CFD models were kept simple by using it only to model drag for the droplets and the flow of slag with homogeneous slag. Also, the method is computationally intensive and, thus, slow compared to either method by themselves, the increased complexity would have only slowed the simulations down. The simulations with available computer took 6 to 8 weeks to solve.

Table 3
Droplet values used in EDEM.

Parameter	Value
$\rho_{coalescence}$	5100 kg/m^3
$\rho_{reaction}$	4500 - 5200 kg/m^3
inlet$_{cubic/simple}$	0.0086 kg/s
inlet$_{deep}$	0.00015 kg/s
time step	$2 \cdot 10^{-5}$ s
d$_{mean}$	500 μm
standard deviation	0.1
feed size range	0.35-0.65 mm

3.3. DEM model

For the DEM simulations, two different models were created: coalescence and reaction models, as they are the key phenomena that occur when matte droplets settle through slag. According to Stokes' law, the coalescence is the more significant of the two as the terminal velocity of the settling sphere is affected by density and the square of the radius. The equation for the terminal velocity of a sphere in a fluid is

$$v = \frac{2}{9}\frac{\rho_s - \rho_f}{\mu} g r^2 \tag{1}$$

where ρ_s and ρ_f are the densities of the sphere and fluid, respectively, μ is the dynamic viscosity, g is the acceleration due to gravity, and r is the radius of the sphere. In this study, the droplets are assumed settle slowly and, thus, having the shape of spheres.

The coalescence model was simulated with a single material type in EDEM but the reaction model required the use of several different materials; their properties are listed in Table 3. The constant density for the coalescence model was taken from study of Xia et al. [6] while the density curve for the reaction model was calculated from laboratory scale experiment by Wan et al. [10] as presented later in Chapter 3.3.2. The models are described in more detail in separate sections below. The time step in EDEM is based on the Rayleigh time step [11].

3.3.1. Coalescence

Colliding droplets may coalesce, thus increasing the droplet size. Coalescence can be simulated by CFD using parcels, which are a statistical description of a droplet group [6]. Typically, collision frequency and coalescence probability are used to determine whether colliding parcels will coalesce. However, the droplets can be simulated individually using DEM, although additional models are required to take coalescence into account. By simulating each droplet as its own entity, parcels and collision frequency are not needed leading from possibility of contacts to a definite contact.

During every droplet–droplet contact, the coalescence model solves the coalescence probability in Equation (2)[12], which was used as the criterion for whether the droplets coalesce or bounce off of each other as presented in Fig. 4 [13].

$$P_c(d_i, d_j) = \exp\left(-\Psi \frac{\sqrt{0.75(1+\xi_{ij}^2)(1+\xi_{ij}^3)}}{\left(\frac{\rho_d}{\rho_s}+\gamma\right)(1+\xi_{ij})^3}\sqrt{We_{ij}}\right), \tag{2}$$

where Ψ is the order of unity, ξ_{ij} is $\frac{d_i}{d_j}$, ρ_d is the droplet density, ρ_s is the slag density, γ is the coefficient of virtual mass, and We_{ij} is the Weber number. As was used in the original coalescence study [12], the order of unity and coefficient of virtual mass were set to 1 and 0.5, respectively.

If the probability is 50% or more, the droplets are marked for coalescence. Marked droplets no longer interact with each other, allowing them to overlap more than would otherwise be possible. Non-marked droplets still affect the coalescing pair and vice versa. The coalescing droplets grow each time step until they reach 95% of the size of the coalesced droplet. When both droplets have reached the set size, they are deleted, and a new droplet is created at the center of mass of the original droplets. However, the size of the coalesced droplets was calculated from the volume of the original droplets. The volume of the coalesced droplet was equal to the sum of the original volumes. Droplet age was set as average of the coalescing droplets for use with the reaction kinetics model. Also, momentum conservation was taken into account by calculating momentum vectors for the original droplets which would be summed to form the momentum vector for the coalesced droplet. A diagram of the process is presented in Fig. 5. The growth at this point is unrealistic but with overlapping it increases the simulation stability significantly, as dense droplet clusters may experience overly large forces if coalesced droplets are placed at the center of the mass instantaneously. This led to droplet "explosions" or software crashes in simulations using the previous coalescence model version [14].

In addition to the coalescing speed, a limit was also placed on the maximum size of the coalesced droplets, as sufficiently large settling droplets would break into smaller ones. Furthermore, the larger the droplets, the more likely they would deviate from a spherical shape, decreasing the accuracy of these simulations since DEM does not take droplet deformation into account. The size of the coalesced droplet was calculated and, if it was larger than the limit, the droplets would not coalesce in the simulation. The

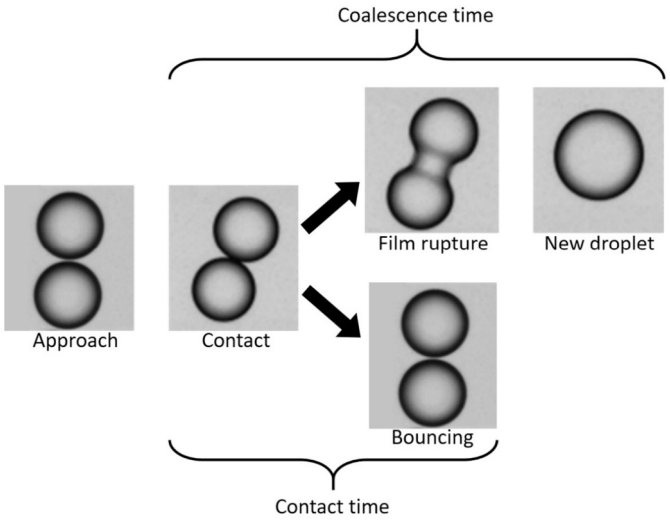

Fig. 4. Droplet contact as presented by Dudek et al. [13].

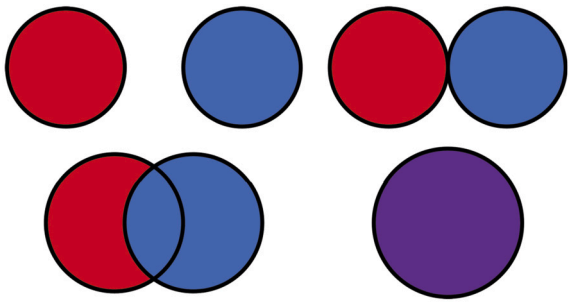

Fig. 5. Behavior of the coalescence model illustrated.

droplet size was limited to 1.5 mm in a simulation with the simple model, 2.0 mm with the cubic model, and up to 40 mm in the deep model. The size limit was increased intermittently as the stability of the simulations was found to be good. However, simulations were not repeated as the simulations took well over a month.

3.3.2. Reaction model

Concentrate oxidation can be generalized to overall reaction (3) [15]. The reaction increases the copper concentration of the matte by removing iron and sulfur, which decreases the size but increases the density of the droplets. As EDEM does not use different compositions or material gradients, separate model and custom properties are needed to simulate reaction-induced changes in droplet properties. These changes are based on in-house measurements by Wan et al. where the Cu, Fe, and S composition or matte were studied [10]. From these measurements, a time-dependent function of the Cu content of a matte droplet can be created:

$$CuFeS_{2(s)} + O_{2(g)} \rightarrow (Cu, Fe, S)_{(matte)} + FeO_{(slag)} + SO_{2(g)} \tag{3}$$

A review by Sundström et al. found a linear relationship for density in the Cu_2S–FeS system (4) [16]. For the reaction model, it was assumed that the sulfur measured by Wan et al. was either found in Cu_2S or FeS and that the reaction only removed FeS, concentrating the Cu in the matte. This allowed calculation of the mass of the sample, enabling the formation of a time-dependent function of matte density. The decrease in droplet size could then be estimated by solving the masses of Cu2S and FeS for a droplet of typical size and then solving the change in FeS mass, as the change of density is known from the previous function. With the known masses and density, the droplet size could be calculated (5). The known sizes were then used to determine the relative change in size and applied to droplets of every size in the simulations.

$$\rho_{Cu_2S-FeS} = 3.9732 + 1.3012 \cdot X_{Cu_2S} \tag{4}$$

$$r = \sqrt[3]{\frac{3(m_{Cu_2S} + m_{FeS})}{4\pi \cdot \rho_{Cu_2S-FeS}}} \tag{5}$$

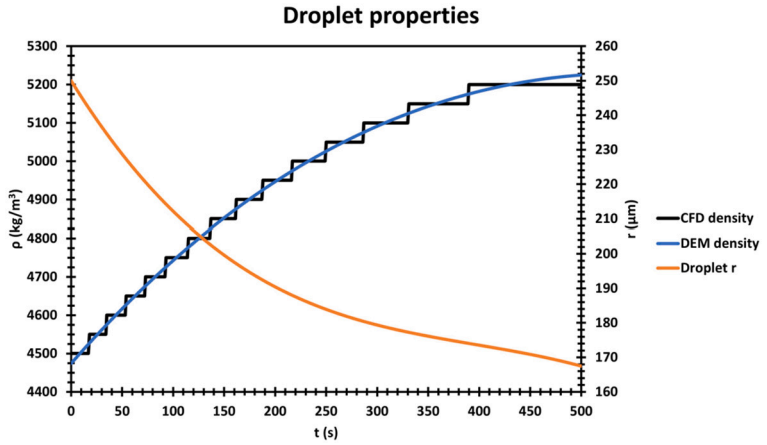

Fig. 6. Properties of a typical droplet in CFD and DEM as a function of droplet age.

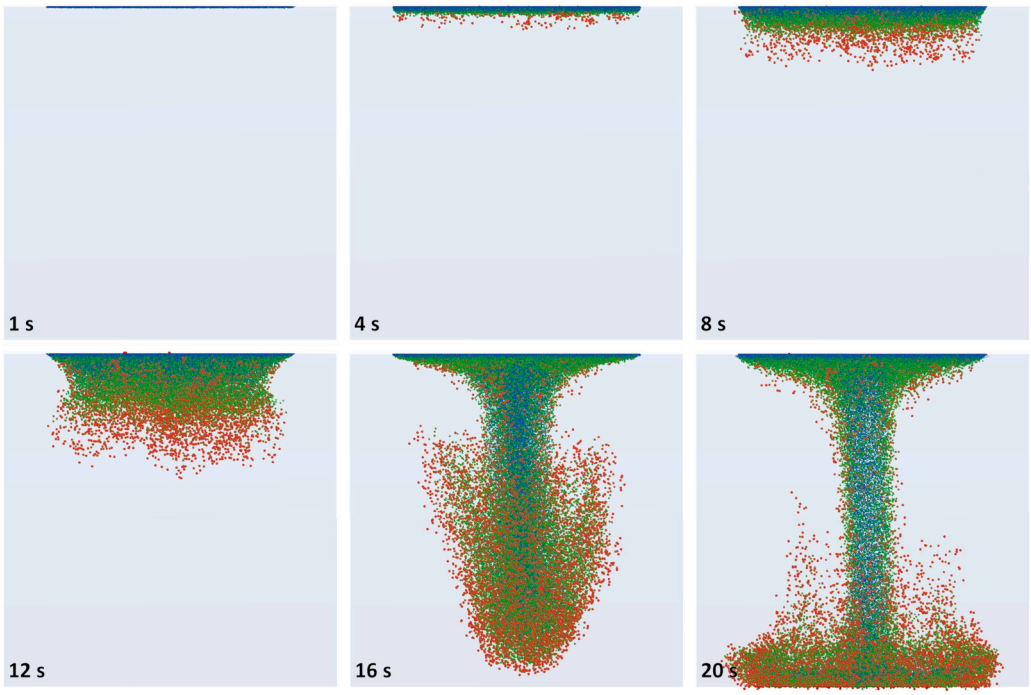

Fig. 7. Channeling flow forming in the simple model.

In EDEM, particles are bound to a material and changing the material would change the properties of every droplet in the simulations. Thus, custom properties were needed to follow the changing droplet age, density, and original scale factor. The droplet age was used to calculate the density and size for each droplet at every time step. However, as EDEM uses material properties in the coupling plugin, different materials were also created. The otherwise identical materials increased in density every 50 kg/m^3 from 4500 to 5200 kg/m^3. If the density of any droplet reached a value which was closer to the next material, the droplet was deleted and a new one was created in its place with the new material. The custom properties of the new droplets were set to the same values as those of the deleted droplet. The properties of the matte droplets are presented in Fig. 6.

The reaction model was designed to be used with a modified coalescence model. As the coalescence model assumes that every droplet has identical properties, custom properties for the original scale factor and age need to be added. The age of the coalesced droplet is set to the weighted average of the droplets based on their volume. The original size of the coalesced droplet is calculated from the original size of the coalescing droplets and then scaled to match the age of the droplet. Scaling calculations are necessary to allow droplet sizes to constantly change while maintaining the size distribution in the feed.

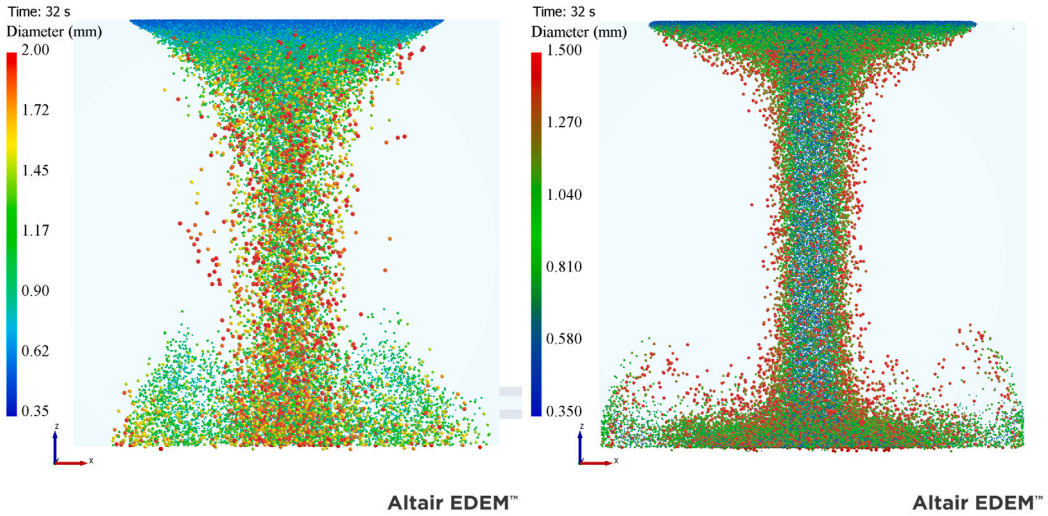

(a) Droplet sizes in the cubic model. (b) Droplet sizes in the simple model.

Fig. 8. Matte droplet diameters in the cubic and simple models.

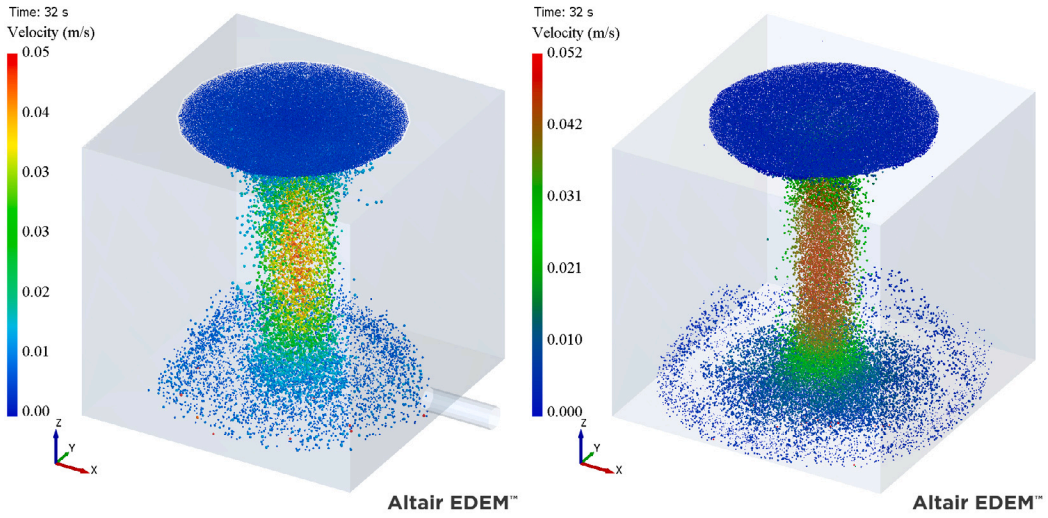

(a) Droplet velocities in the cubic model. (b) Droplet velocities in the simple model.

Fig. 9. Matte droplet velocities in the cubic and simple models.

4. Results

4.1. Coalescence

In the simulations, droplets started to coalesce close to the slag surface as the drag caused droplets to slow down and collide, and also as the droplets were pushed into a denser cluster by the channeling phenomenon. The coalesced droplets settled faster than other droplets due to their increased size. The settling droplet cluster induced flow in the slag which created a ring where the slag flowed downwards in the middle and up near the outer edges. This, in turn, pushed the cluster more toward the centerline, which increased contact between droplets and, thus, increased the coalescence rate. The flow also pulled the droplets faster through the slag than they would have settled without it. Formation and behavior of the channeling flow is presented in Fig. 7. This channeling or funneling phenomenon has also been observed with a large-scale CFD simulation where several channels formed [14]. The channeling phenomenon and flow in the slag in the cubic and the simple models are presented in Figs. 8, 9, 10. From Figs. 8b, 8a, it can be seen that both the simple and the cubic models reached the set maximum sizes for coalesced droplets. However, the general shape of the channel and the flow field are similar.

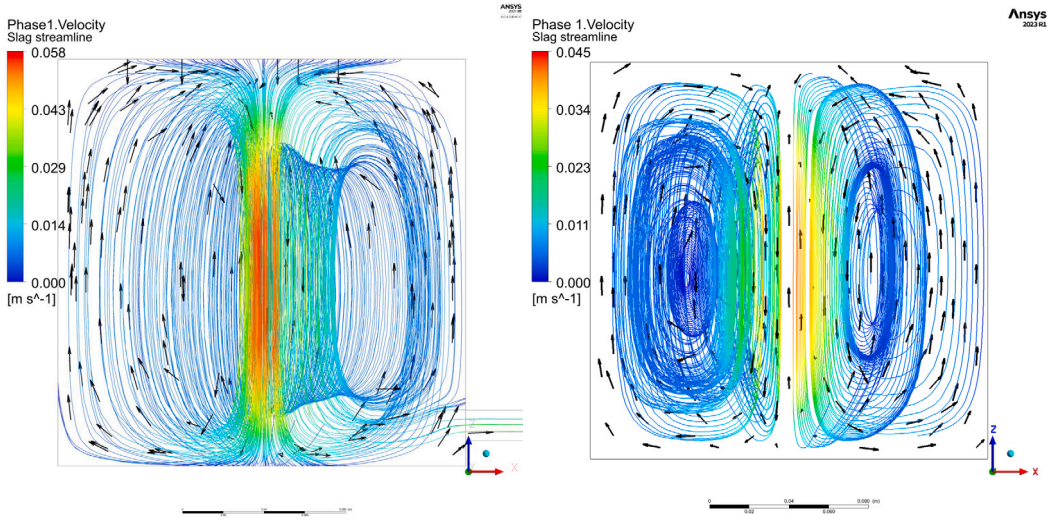

(a) Slag flow in the cubic model. (b) Slag flow in the simple model.

Fig. 10. Slag flows in the cubic and simple models.

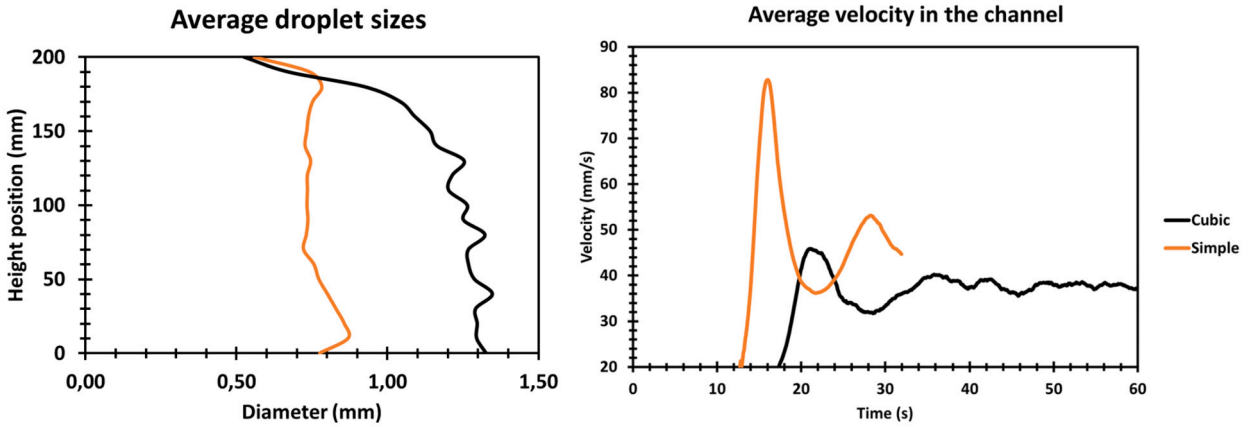

Fig. 11. Average droplet sizes and average droplet velocity at the center of the model.

Velocity profiles of the slag, presented in Figs. 10b and 10a, are also similar, although the simple model shows a slightly faster flow in the formed channel. The highest velocity in the models is in the middle of the channel, except for the droplets that pass through the model geometry and fall without drag. However, as can be seen in Fig. 11, the velocities inside the channel fluctuate cyclically but stabilize in the cubic model. They have not yet stabilized in the shorter simple model. The more sharply defined channel in the simple model causes the velocity to form a narrower and higher peak and the cluster to reach the middle point of the model faster than in the cubic model.

Even though both models produced a similar channeling effect, the cubic model did not produce as tight and symmetrical a channel as the simple model. Also, the droplets seemed to coalesce to a greater degree close to the surface in the simple model. The earlier coalescence was caused by the flow from the fed slag pushing the matte droplets faster, leading to a less dense droplet cluster in the cubic model. This can also be seen in Fig. 11 where the average diameter of the matte droplets in the simple model grew faster than in the cubic model. However, the size limit can be seen in the simple geometry curve as the average size stopped growing abruptly while the cubic model curve growth decelerated much more smoothly. A comparison of the diameters in the same size scale is presented in Fig. 12.

Slowing down the coalescence phenomenon in the simulation by allowing the coalescing droplets to overlap and grow before creating a new one made the simulations more stable. With the previous model, several droplets could coalesce into one practically instantly, as presented in Fig. 13. This multiple coalescence was not a problem provided that other droplets were not too close. If other droplets were too close, the coalesced droplet could overlap with the other droplets too much, resulting in the calculated normal forces being excessively high, in which case the droplet cluster would explode.

The new model did not show any explosive behavior as the coalescing droplets pushed neighboring droplets aside. This also slowed down the coalescence phenomenon from instantaneous to a longer event, which could also slow down the overall coalescence rate.

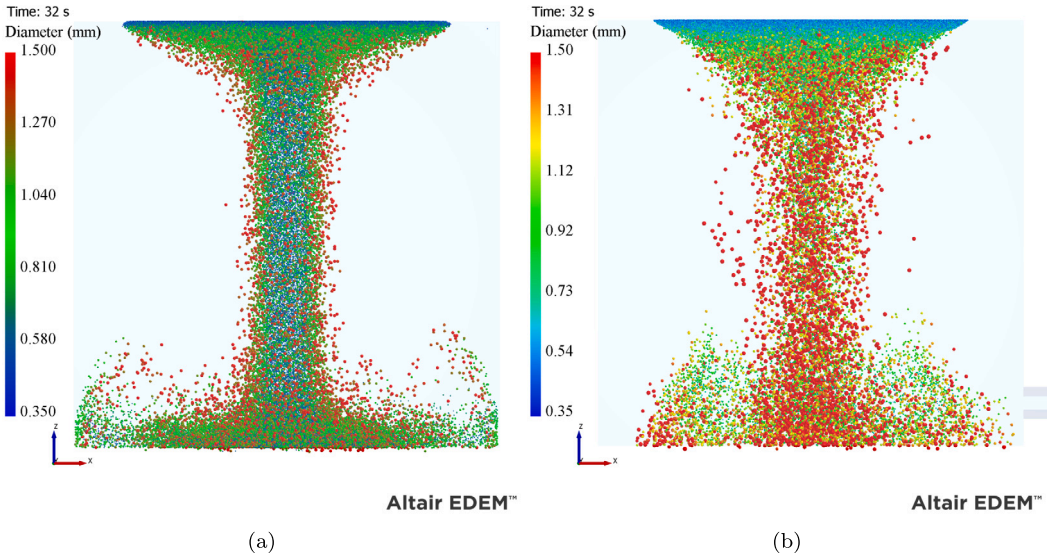

Fig. 12. Droplet sizes at the same simulated time and size scale in the (a) simple and (b) cubic models.

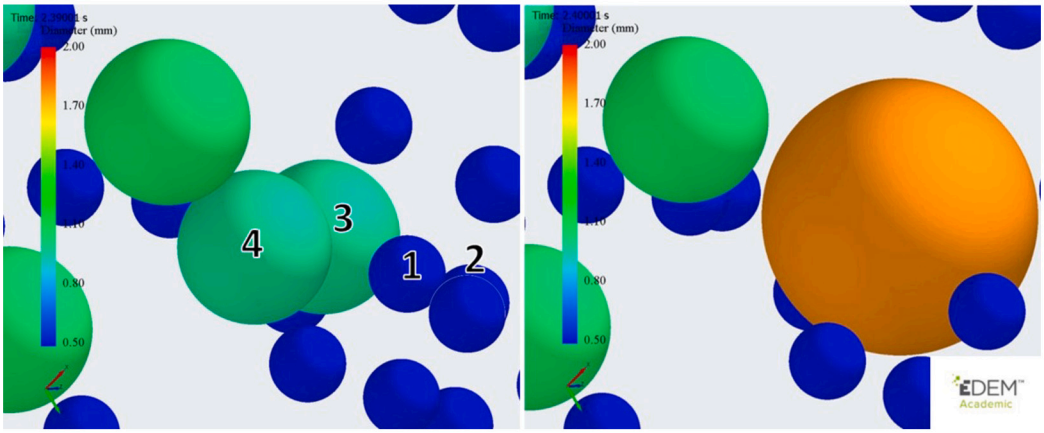

Fig. 13. Several droplets coalescing simultaneously. [9].

An example of coalescence with the new model is presented in Fig. 14, where droplet 1 grows between frames 1 and 2 but then reaches the size criterion (95% of the size of the coalesced droplet); the droplets coalesce only when droplet 2 also reaches the same criterion. The formed droplet is close to the maximum size set for the simulation.

In the simulations, the number of droplets reaches a relatively steady state as some of the droplets coalesce and some settle through the slag and are removed. These steady state numbers are 125 000 and 130 000 droplets for the cubic model and the simple model, respectively. As presented in Fig. 15, the simple model has a slightly higher droplet count even though the number of uncoalesced droplets is higher and the settling velocity is significantly lower in the cubic model, as can be seen in Fig. 16. The number of uncoalesced droplets varied at first as the channeling flow was forming and densifying the cluster which caused the number to decrease. When the channel had formed and penetrated the slag layer, the number of droplets in the simulation stabilized and the droplets were coalescing in a relatively predictable amounts as was shown in Fig. 11.

4.2. Combined model

The combined model with both coalescence and reactions behaved similarly to the coalescence models even though the droplets were injected in a much smaller inlet area. The channeling effect was more prominent near the slag surface compared to the effects in the cubic and simple models. Larger droplets could be seen forming already near the surface. In Figs. 17a, 17b and 18, droplets can be seen coalescing already very close to the slag surface where the coalescence rate can be seen to increase as larger droplets start to form when the flows pull the settling cluster closer toward the centerline. However, after the droplets enter the channel, the coalescence rate decreases rapidly as the droplets collide less with each other. This can be seen in the relatively stable average droplet size. As the largest droplets settle faster, the lowermost droplets are large in size and the average size increases significantly.

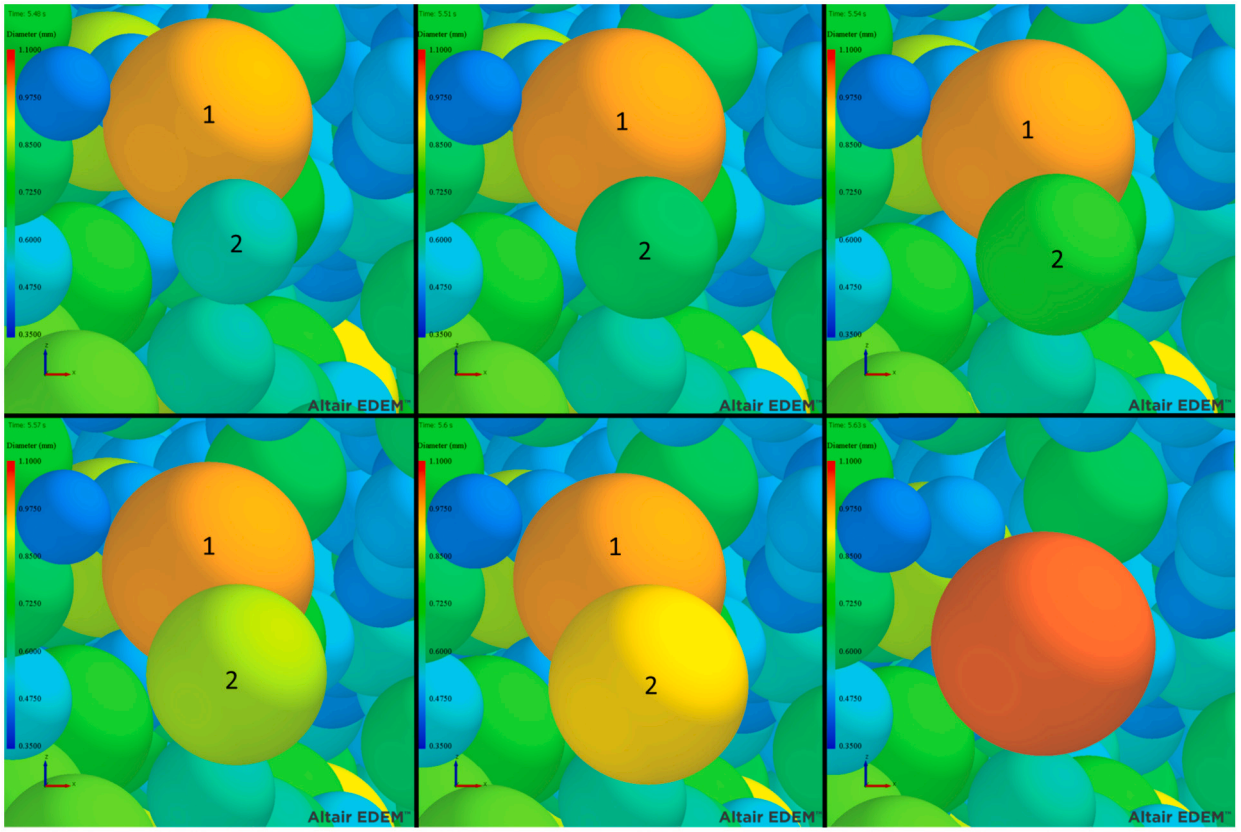

Fig. 14. Coalescence of two different-sized droplets.

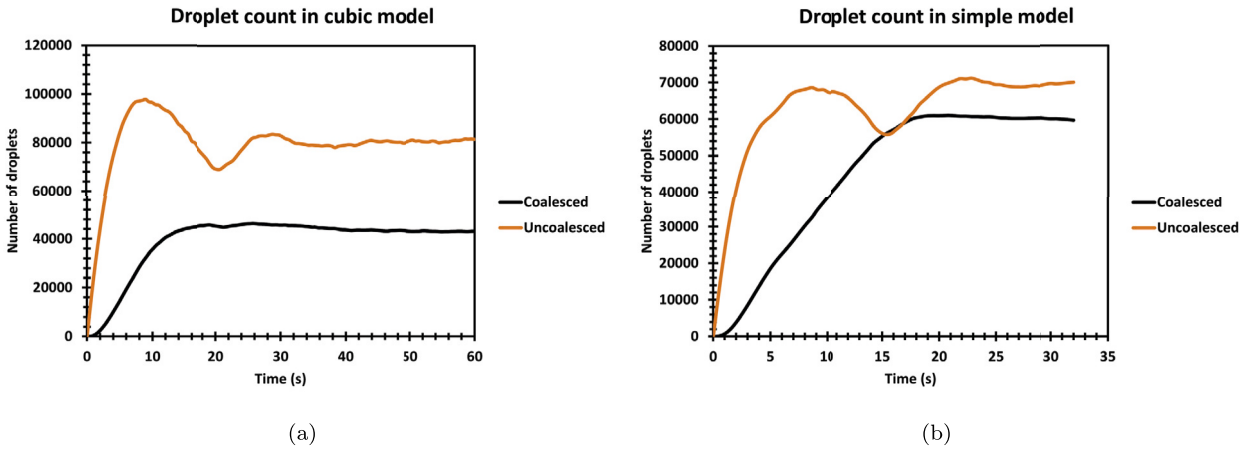

Fig. 15. Numbers of coalesced and uncoalesced droplets in the (a) cubic and (b) simple models.

The first droplets fed to the simulation started to settle straight down as the channel had not yet formed. Some of the droplets were on the outer edge of the channel and were not pulled to the centerline of the cluster and did not coalesce with other droplets. This created a rim around the channel which cannot be observed in the simple or cubic models. However, the rim can be seen in Fig. 19.

The rim can also be seen when the droplet densities are plotted as a function of their height coordinate, as shown in Fig. 20. The curve shows the relatively linear progress of the droplets although the group becomes more dispersed the further down the droplets are. This was caused by droplets of different densities and sizes coalescing. The coalescence occurred as a larger droplet settled faster and collided with a smaller droplet. The smaller droplet was older and thus denser, as it had more time to react with the slag. Coalescence between droplets of different densities curves the plotted group toward a slightly slower reaction rate, which

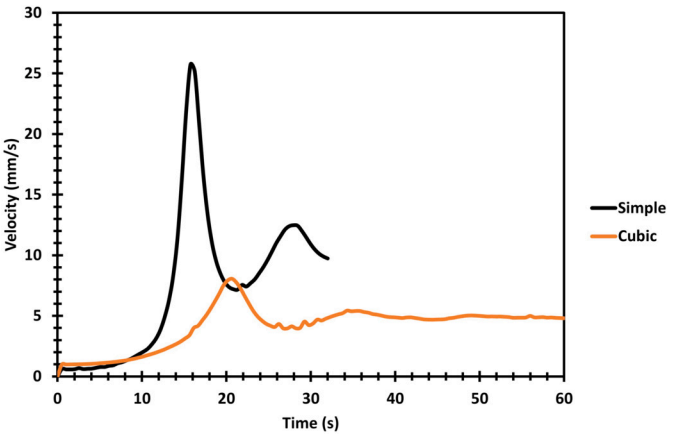

Fig. 16. Average settling velocities in the simple and cubic models.

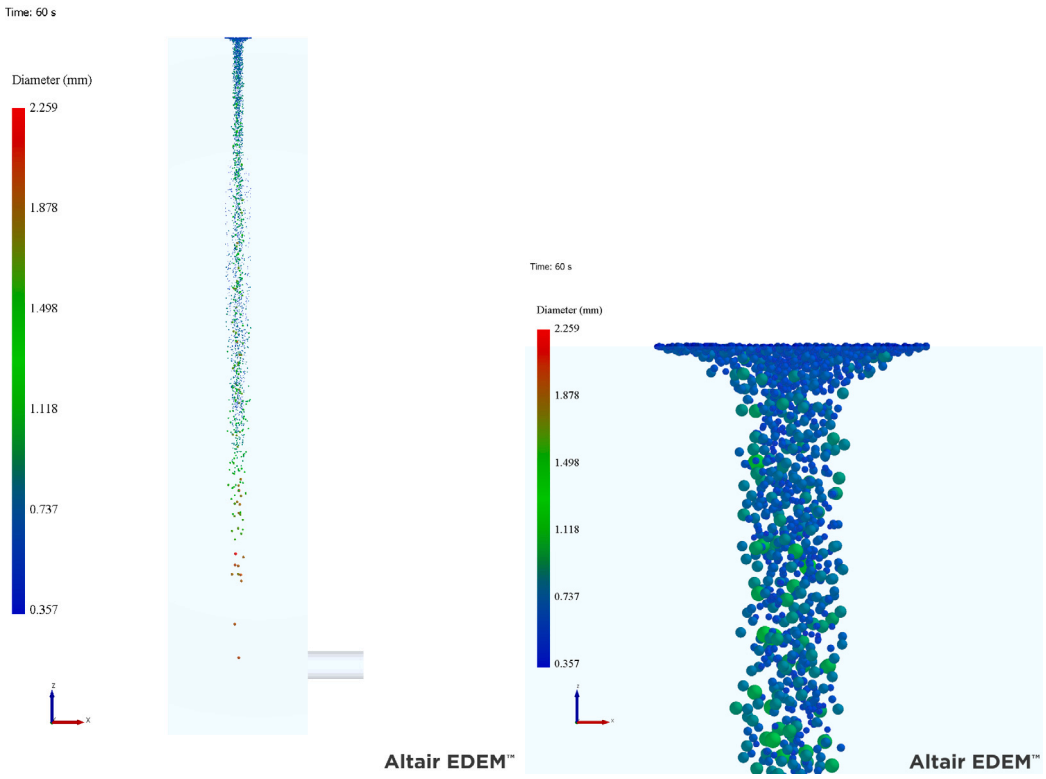

(a) Full model. (b) Close-up of the slag surface.

Fig. 17. Droplet diameters in the deep model.

can be seen in the fixed trendline. In the fixed trendline, droplets forming the rim were removed. The rim can also be seen in the height–velocity graph in Fig. 21a as one tight group does not fit the formed curve. The Fig. 22 also shows that droplet velocities in the deep model are highest in the channeling flow, similarly to the cubic and simple models. However, in the deep model, the highest velocity was not in the middle of the model but instead fairly close to the slag surface. Still, the average settling velocity of the droplets stabilized similarly to the cubic and simple models as can be seen in Fig. 21b.

5. Discussion

The decelerated coalescence of the new model is a significant improvement over the older one in terms of simulation stability, as it allows simulation of denser droplet clusters. Furthermore, it can be argued that the slower coalescence of two droplets is more

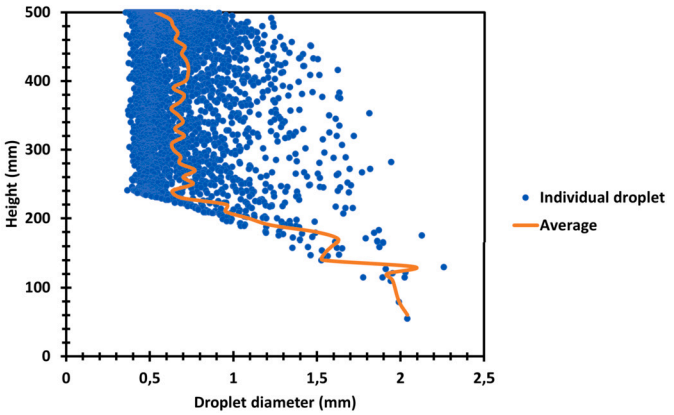

Fig. 18. Droplet sizes in the deep model at 60 s.

realistic than practically instantaneous coalescence, as real droplets have mass and inertia and thus need time to move. Also, the improved reaction model created a gradient of different densities, which is a significant improvement over the layered structure created by the previous version [9]. The gradient of the different states of the droplets becomes increasingly important as more models are combined. Stepped changes in density, for example, would cause a stepped acceleration for the settling droplets, and also cause inaccuracy in determining whether colliding droplets would coalesce.

The channeling effect was formed in every simulation and seems to be one of the key mechanisms affecting matte settling through slag. The channel is created by the settling droplets and seems to be affected by other flow-inducing mechanisms such as feed and most likely tapping. A slightly uneven feed could disrupt the flow and cause formation of multiple channels, as observed in the previous study.

The difference between the cubic and simple models is caused by the added slag flow and also the size limit for the droplets. However, the difference is probably not very significant as the droplets in the deep model did not grow into droplets that were much larger than in the more limited models. The cluster should be relatively similar in density in every simulation, especially near the surface. The cluster density decreases in every model toward the matte—slag interface but it is more pronounced in the deep model as the cluster is thinner and the geometry is significantly deeper. The cluster is densest in the simple model, which is due to having more droplets than in the other two simulations.

The difference between droplet numbers in the cubic and the simple models is probably caused by the size limit. As the simple model has a lower size limit, some of the droplets did not coalesce even though the criterion would have otherwise been met. On the other hand, more uncoalesced droplets were present in the cubic model but the coalesced droplets were able to coalesce several times, resulting in lower total droplet numbers.

In the combined model, a rim of smaller and denser droplets remained around the channel. This was most likely caused by having a small inlet area leading to a narrow channel. With such a narrow channel, the slag flow did not push the droplets at the rim toward the centerline but flowed vertically downward and thus the smaller droplets never collided and coalesced. Furthermore, the channel seems to spread slightly toward the bottom. The spreading was probably caused by the settling not having yet reached a relatively steady state. However, the settling velocity seemed to have reached a steady state.

The unreached steady state was also the probable cause for the fact that the velocity field differed from the cubic models. A significantly longer simulation would have been needed to study whether such a steady state would have been reached but such long simulations were not a viable option with the computational power available.

6. Conclusions

The CFD-DEM method provides a valuable tool for studying the flash smelting settler previously unobtained level of detail. The method is valuable tool for research and process development, as it is practically impossible to directly observe the matte inside the slag layer. Several different submodels are needed to simulate the different phenomena in the slag. At this stage, coalescence and reaction models have been developed and refined for modifying settling matte droplets. The CFD-DEM method is computationally too intensive for simulating full-sized flash smelting processes in any realistic time period. However, with suitable models, the method is a capable tool for studying different phenomena occurring in the furnace by using smaller-scale models. Large-scale models are not practically viable options with current desktop computers as even these models require one to two months of calculation time per minute of simulated time.

Both coalescence and combined coalescence-reaction models produce a channeling phenomenon in the slag. The phenomenon is emphasized more by the closeness of the walls in the deep geometry. As such a phenomenon has been observed in several different models with CFD-DEM and also with a full-scale CFD model, the results seem fairly reliable. Therefore, a practical validation study is the next step as channeling significantly increases the settling velocity of droplets. More practical studies could also be considered for refining the reaction rate and coalescence criteria. However, observations even in a small scale will be difficult at best. Also, developing new models for loss mechanisms, such as spinels, should be considered.

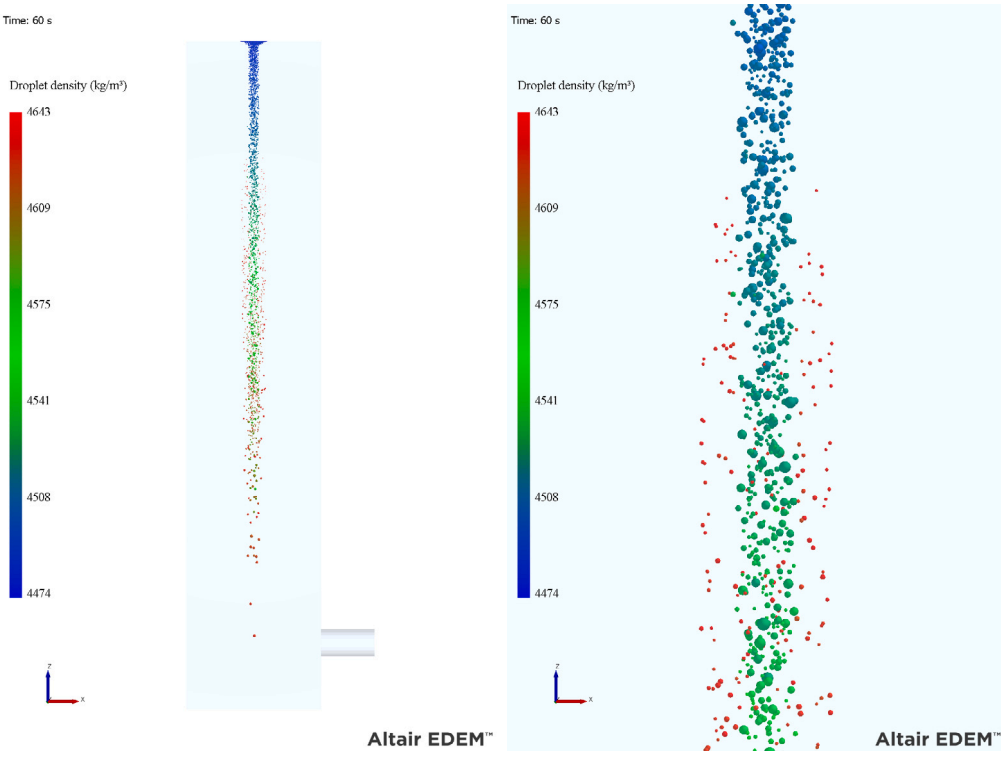

(a) Full model. (b) Middle of the channel.

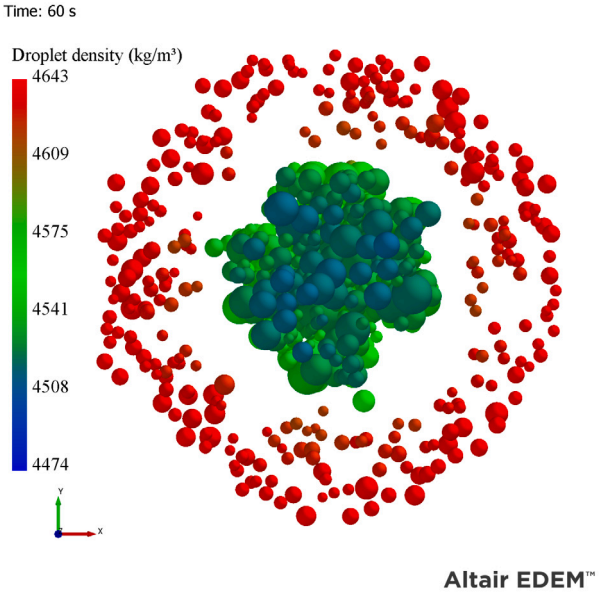

(c) 100 mm tall slice from the middle of the cluster showing the rim.

Fig. 19. Droplet densities in the deep model showing the rim.

For large-scale simulations, much more computational power and memory are needed. Simulating a full-sized FSF process would also mean simulating hundreds of millions or even billions of droplets. Every calculation would be performed on every droplet while requiring enough memory for the default data as well as for the custom properties used by the submodels. Such simulations could be achievable with supercomputers but focusing on smaller scale models is the most practical option at the time of writing this article.

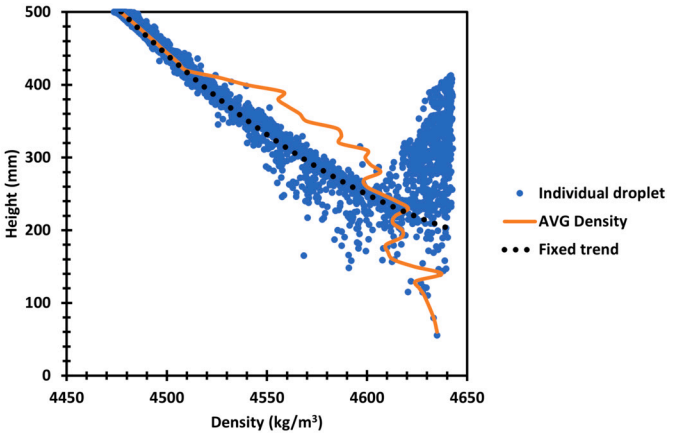

Fig. 20. Droplet densities in the deep model at 60 s.

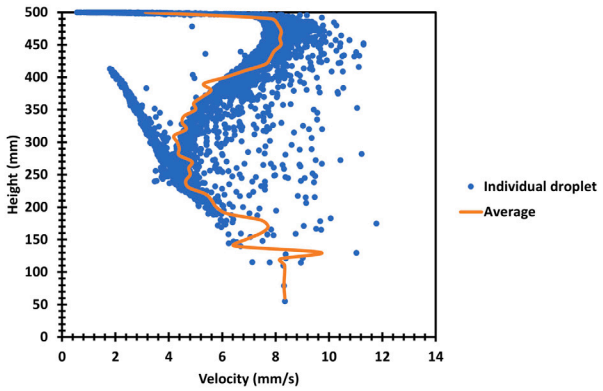

(a) Settling velocity of droplets in the deep model at 60 s.

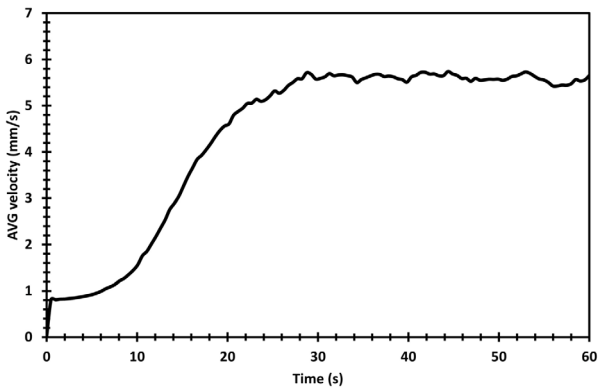

(b) Average settling velocity of the droplets.

Fig. 21. Droplet velocities in the deep model.

More research is needed to study the creation mechanisms of the channeling effect and the effect of the closeness of the walls in the simulation. Such work could validate the findings made in this project. Also, future simulations would benefit from additional submodels for taking spinels into account and also for using reaction models in Fluent and tying them to the reaction model for droplets.

Ethics declarations

Review and/or approval by an ethics committee was not needed for this study because this study simulates phenomena in an industrial smelting process using computer simulations.

CRediT authorship contribution statement

Jani-Petteri Jylhä: Conceptualization, Data curation, Formal analysis, Investigation, Methodology, Software, Validation, Visualization, Writing – original draft, Writing – review & editing. **Ari Jokilaakso:** Funding acquisition, Project administration, Resources, Supervision, Writing – original draft, Writing – review & editing.

Declaration of competing interest

The authors declare that they have no known competing financial interests or personal relationships that could have appeared to influence the work reported in this paper.

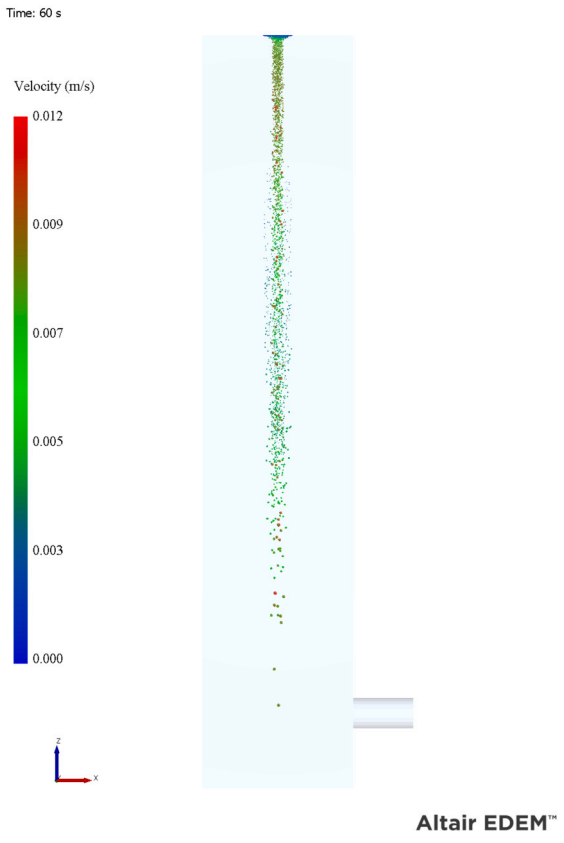

Fig. 22. Velocities of the settling droplets.

Data availability

Data has not been deposited into a publicly available repository but will be made available on request.

Acknowledgements

The authors would like to acknowledge the financial support from Business Finland as this work has been a part of the TOCANEM project. Grant number: 41778/31/2020.

References

[1] R. Sridhar, J.M. Toguri, S. Simeonov, Copper losses and thermodynamic considerations in copper smelting, Metall. Mater. Trans., B Process Metall. Mater. Proc. Sci. 28 (2) (1997) 191–200, https://doi.org/10.1007/s11663-997-0084-5.

[2] P. Taskinen, K. Seppälä, J. Laulumaa, J. Poijärvi, Oxygen pressure in the Outokumpu flash smelting furnace—part 1: copper flash smelting settler, Miner. Process. Extr. Metall. 110 (2) (2001) 94–100, https://doi.org/10.1179/mpm.2001.110.2.101, http://www.tandfonline.com/doi/full/10.1179/mpm.2001.110.2.101.

[3] W.G. Davenport, E.H. Partelpoeg, Flash Smelting: Analysis, Control and Optimization, Elsevier Science, New York, 1987, pp. 22–28.

[4] M.E. Schlesinger, M.J. King, W.G. Davenport, Extractive Metallurgy of Copper, Elsevier Science, 2011, https://books.google.fi/books?id=sXcorPHuHowC.

[5] J. Xia, T. Ahokainen, T. Kankaanpää, J. Järvi, P. Taskinen, Numerical modelling of copper droplet setting behavior in the settler of a flash smelting furnace, in: Proceedings - European Metallurgical Conference, EMC 2005, Dresden, 2005.

[6] J.L. Xia, T. Ahokainen, T. Kankaanpää, J. Järvi, P. Taskinen, Flow and heat transfer performance of slag and matte in the settler of a copper flash smelting furnace, Steel Res. Int. 78 (2) (2007) 155–159, https://doi.org/10.1002/srin.200705873, http://doi.wiley.com/10.1002/srin.200705873.

[7] N.A. Khan, A. Jokilaakso, Dynamic modelling of Molten slag-matte interactions in an industrial flash smelting furnace settler, in: Extraction 2018, Springer International Publishing, Cham, 2018, pp. 993–1005.

[8] N.A. Khan, A. Jokilaakso, Flash smelting settler design modifications to reduce copper losses using numerical methods, Processes 10 (4) (2022), https://doi.org/10.3390/pr10040784, https://www.mdpi.com/2227-9717/10/4/784.

[9] J.-P. Jylhä, A. Jokilaakso, CFD-DEM modelling of matte droplet behaviour in a flash smelting settler, in: Proceedings of the 58th Conference of Metallurgists Hosting the 10th International Copper Conference 2019, 2019, pp. 1–15.

[10] X. Wan, L. Shen, A. Jokilaakso, H. Eriç, P. Taskinen, Experimental approach to matte–slag reactions in the flash smelting process, Miner. Process. Extr. Metall. Rev. 42 (4) (2021) 231–241, https://doi.org/10.1080/08827508.2020.1737801.

[11] Altair Engineering Inc., EDEM 2022.3 User Guide, https://2022.help.altair.com/2022.2/EDEM/Simulator.htm, 2023.

[12] T. Wang, J. Wang, Y. Jin, Theoretical prediction of flow regime transition in bubble columns by the population balance model, Chem. Eng. Sci. 60 (22) (2005) 6199–6209, https://doi.org/10.1016/j.ces.2005.04.027.

[13] M. Dudek, D. Fernandes, E. Helno Herø, G. Øye, Microfluidic method for determining drop-drop coalescence and contact times in flow, Colloids Surf. A, Physicochem. Eng. Asp. 586 (2020) 124265, https://doi.org/10.1016/j.colsurfa.2019.124265, https://www.sciencedirect.com/science/article/pii/S0927775719312609.

[14] J.P. Jylhä, N.A. Khan, A. Jokilaakso, Computational approaches for studying slag-matte interactions in the flash smelting furnace (FSF) settler, Processes 8 (4) (Apr 2020), https://doi.org/10.3390/PR8040485.

[15] P.I. Guntoro, A. Jokilaakso, N. Hellstén, P. Taskinen, Copper matte - slag reaction sequences and separation processes in matte smelting, J. Min. Metall., B Metall. 54 (3) (2018) 301–311, https://doi.org/10.2298/JMMB180214021G.

[16] A.W. Sundström, J.J. Eksteen, G.A. Georgalli, A review of the physical properties of base metal mattes, J. S. Afr. Inst. Min. Metall. 108 (8) (2008) 431–448.